

MEMS for Drug Screening Applications

J. Zhou*, S. Zurn*, D. Markus*, S. Mantell*, D. Polla* and G. Smith**

*University of Minnesota, Minneapolis, MN, USA, smantell@me.umn.edu

**Affymax, Mountain View, CA

ABSTRACT

MEMs sensors have the potential to serve as a low cost method for screening new drugs. To examine the feasibility of this technique, microbeams were designed such that an affinity between the beam surface (coated with a biomolecule) and a second biomolecule (simulating a potential drug) created a shift in the beam resonant frequency. PZT-actuated cantilever and bridge microbeams were fabricated and a baseline resonant frequency was established for each beam. Avidin and biotin were attached to the microbeams through a series of immersion and drying steps. Subsequent changes in the resonant frequency were recorded and compared for each beam. A drop in resonant frequency was consistently noted after the biotin molecule was introduced. To verify that the frequency shift could be attributed to the added mass of biotin, a biotin molecule with fluorescein dye was introduced. A direct correlation between fluorescent intensity and resonant frequency shift was observed.

Keywords: microbeam, resonant frequency, drug screening, Avidin, Biotin

1 INTRODUCTION

One novel application for MEMs devices is in drug screening. Using combinatorial chemistry, many new compounds (potential drugs) can be synthesized. Effectiveness of the potential drug is determined by whether or not it reacts with a particular biomolecule (representing a bacteria or virus). Thus, a rapid, low cost method for screening compounds is desirable. The screening technique must be capable of detecting the changes associated with bonding between two compounds. These changes can include a change in weight (mass), volume, shape, electrical and thermal properties.

In recent years, there has been an increasing interest in the development and application of microcantilever sensors because of their potential to present considerably higher sensitivity than other microsensors [1]. Microcantilevers were utilized as sensors following two approaches: static and dynamic [1-3]. In the static approach, displacement induced stresses are caused by temperature changes, and molecular interactions. For example, researchers have measured beam displacements on the order of 10 nm (1 μ m x 500 μ m x 100 μ m beams) in cantilevers that have been

covered with biomolecules. In the dynamic approach, frequency shifts associated with variations in mass and/or stiffness are induced. The dynamic sensing approach has been applied to large beams, that are characterized by a relatively high mass/surface area ratio and stiffness/surface area. These large, stiff beams would not suffice for measuring the small changes in mass and stiffness associated with a layer of biomolecules attracted to the beam surface.

MEMs beams, on the other hand, have a much lower mass. The added mass of the biomolecule layer may be sufficient to shift the resonant frequency of a MEMs beam. The focus of this paper is to describe the design and evaluation of a MEMs microbeam specifically designed to sense changes in mass on the molecular level. In this study, attraction in a well-characterized biomolecule pair, avidin-biotin, was investigated. In subsequent sections, microbeam design and performance are presented.

2 MODEL

In order to predict the performance of a microbeam based sensor, the beam resonant frequency and shift in resonant frequency (for an added mass) must be evaluated. Typical MEMs microbeams should be modeled as plates, since the length a and width b are much larger than the thickness t . The resonant frequencies f_{ij} for a plate vibrating in air are:

$$f_{ij} = \frac{\lambda_{ij}}{2\pi a^2} \left(\frac{Et^3}{12\gamma(1-\nu^2)} \right)^{0.5} \quad (1)$$

where γ and E are the mass per unit area and the Young's modulus of the plate, respectively. The dimensionless parameter λ_{ij} is a function of the vibration mode indices (i, j), the Poisson's ratio ν , the plate geometry, and the boundary conditions on the plate. These constants are tabulated in [4] for plates that are supported at one end (cantilever) and both ends (bridge).

Because the plate is comprised of n layers, an equivalent modulus E_{eq} must be calculated following a rule of mixtures approach:

$$E_{eq} = \sum_{i=1}^n E_i t_i \quad (2)$$

where t_i is the thickness of the i^{th} layer.

The effect of adding biomolecules to the microstructure is a change of its effective mass and, hence, a shift in the resonance frequencies. By applying equation (1) to the case where a mass has been uniformly distributed on the surface with a mass distribution γ_a , the shift in resonant frequency Δf can be determined:

$$\frac{\Delta f}{f} = \sqrt{\frac{\gamma}{\gamma + \gamma_a}} - 1 \quad (3)$$

The percentage change in frequency $\Delta f/f$ depends only on the ratio of added mass to the mass of the beam. It is independent of the frequency and of the structure, bridge or cantilever. Thus, given the same plate geometry and materials, a bridge design will be stiffer than a cantilever design, resulting in higher resonant frequencies and numerically larger frequency shifts.

Also of critical importance in designing the microbeam is the relationship of the actuating PZT layers relative to the beam neutral axis. The actuating layer should be as far away from the neutral axis as possible so as to elicit the largest displacement. A technique for calculating the neutral axis for layered materials is described in [4] and not reported herein.

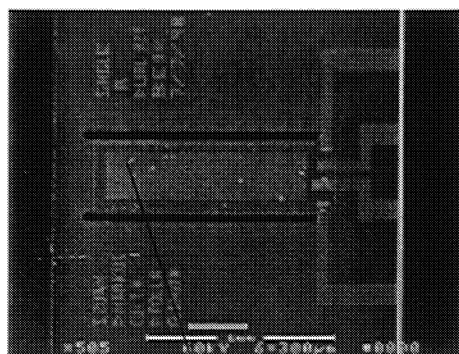
3 EXPERIMENTAL METHODS

3.1 Microbeam design

Cantilever and bridge microbeams were fabricated at the Microtechnology Laboratory at the University of Minnesota. Beam materials, layering sequence and thickness are shown in figure 1. Overall size of the beams was 300 μm wide by 1000 μm long. The backside of the wafer was removed by deep reactive ion etching to free the microbeams from the wafer. With the exception of the PZT layers, layers were deposited and etched following standard MEMS surface machining techniques. A gold surface was deposited on the beam to enhance the biomolecule attachment to the beam. Two PZT layers are included: one for sensing and one for actuating. The PZT layers were spun on using a sol-gel process developed at the University of Minnesota [5].

3.2 Surface chemistry

A two step protocol was developed to introduce a biomolecule to the microbeam (Tables 1 and 2). In general, the protocol involved binding avidin to the cleaned gold surface. To amplify the change in resonant frequency, biotin with BCIP or biotin with fluorescein dye was linked to the avidin. Frequency data were recorded initially, after binding avidin, and after binding the biotin/BCIP or Biotin/fluorescein.



Au	(0.5 μm)
SiO ₂	(0.5 μm)
Ti	(0.1 μm)
Pt	(0.1 μm)
PZT	(0.4 μm)
Pt	(0.1 μm)
PZT	(0.4 μm)
Pt	(0.15 μm)
Ti	(0.015 μm)
SiO ₂	(0.5 μm)

Figure 1: Layer sequence for microbeam. The bridge microbeam is shown.

Solution	Operation
0.2mg/mL Avidin in PBS	Immerse device for variable time
0.75mg/mL biotin-alkaline phosphatase conjugate	Immerse devices for 30min.
50mM Tris buffer (pH=7.4)	Rinse device
1.15mM BCIP	Immerse devices for 30-45min

Table 1: Two-Step Protocol with Biotin/BCIP

Solution	Operation
0.2mg/mL Avidin in PBS	Immerse device for variable time
0.75mg/mL biotin-alkaline phosphatase conjugate	Immerse devices for 30min.
50mM Tris buffer (pH=7.4)	Rinse device
1mg fluorescein in 10mL DMSO diluted with PBS (pH=7.4) 2x	Immerse devices for 2hrs.

Table 2: Two-Step Protocol with Biotin/fluorescein

3.3 Resonant frequency

The resonant frequencies of the microbeams were determined by driving one PZT layer at a constant amplitude over a range of frequencies. The swept frequency

range was from 10kHz to 150kHz. During this frequency scan, the output voltage of the second PZT layer was recorded. Data were acquired using an impedance analyzer (HP-4194A) or a vector signal analyzer (HP-89410A). The source voltage for the impedance analyzer was 0.01 V and for the vector analyzer 0.5 V. Peaks in the sensing PZT output voltage indicated resonant frequencies of the beams.

3.4 Measuring added mass

The biomolecule mass was measured indirectly by noting the shift in resonant frequency following the introduction of the various biomolecule solutions. The presence of the avidin/biotin pair was also “quantified” by observing the fluorescence of the beams that had been immersed in the biotin/fluorescein solution. A fluorescent microscope with digital image analysis software was used to compare beams that had been immersed in the avidin/biotin/fluorescein solution (two step protocol) with control beams. The relationship between the shift in resonant frequency (after avidin/biotin/fluorescein is introduced onto the beam surface) and the fluorescent intensity indicates the microbeam sensitivity to the added mass of this layer.

4 RESULTS & DISCUSSION

4.1 Resonant frequency

Resonant frequency data for “clean” (i.e. no biomolecule) microbeams is summarized in Table 3. In all 28 cantilever and 35 bridge microbeams were tested. Typical resonant frequency sweep data for a bridge structure are shown in figure 2. Figure 3 shows a histogram of resonant frequency data for bridge microbeams. As shown in the histogram, there is some variation in resonant frequency from device to device. This variation is acceptable for this application because the relative change in resonant frequency for a particular device is the indicator of added mass. Similar results were obtained for the cantilever microbeams.

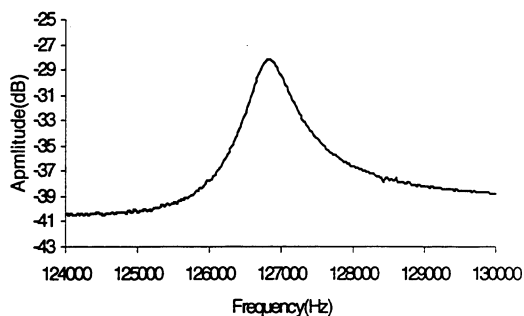


Figure 2: Typical resonant frequency sweep data for a bridge microbeam.

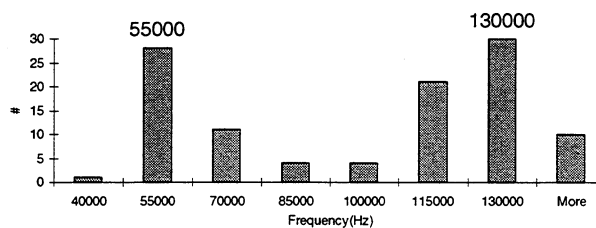


Figure 3: Histogram of resonant frequency data for bridge microbeams. Thirty-five beams in all were tested.

Theoretical values for resonant frequency are also included in Table 3. Table 4 contains a listing of material properties used in calculating the equivalent modulus and plate density required for the theoretical calculation of resonant frequency. The mode constants λ_{ij} for a plate with geometry ratio $a/b=3.33$ are summarized for the cantilever and bridge structure in Table 5.

Table 3: Theoretical and experimental values for resonant frequency.

Sensor frequency (Hz)	Cantilever		Bridge	
	data	model	data	model
f_1	1,700	1,400		9,700
f_2	8,900	8,750		26,718
f_3	30,500	24,539	55,000	52,397
f_4	52,000	48,125		86,607
f_5	88,100	79,545	130,000	129,478

Table 4: Material properties used in calculating the equivalent modulus and plate density required for the theoretical calculation of resonant frequency.

Material	E (GPa)	Density (kg/m ³)	Poisson's ratio	Thickness (μm)
Au	78	19300	0.44	0.5
Ti	120	4510	0.32	0.115
Pt	170	21090	0.38	0.35
PZT	120	7700	0.31	0.8
SiO ₂	60	2190	0.25	1
equivalent	95	9239	0.3	2.765

Table 5: The mode constants λ_{ij} for a plate with geometry ratio $a/b=3.33$ and $\nu=0.3$.

mode	1	2	3	4	5
Cantilever	3.5	18.0	21.6	57.5	60.6
Bridge	22.1	41.7	61.0	92.4	119.9

Data were obtained for the first five resonant frequencies of the cantilever microbeams. In contrast, only the 3rd and 5th resonant frequencies could be detected for the bridge structures. Because bridge structures are stiffer, the deflection and subsequently PZT output will be less than in the cantilever beams. This difference in stiffness could account for the limited resonant frequency data. On the other hand, resonant frequency data for bridge devices have better agreement with theoretical values than frequency data for the cantilever devices. Because one end is free in a cantilever, residual stresses induced during fabrication often lead to curved structures. This curvature can affect the beam resonant frequency. Resonant frequencies for a curved structure are higher than those of a flat plate [4].

4.2 Change in resonant frequency with added mass

A typical frequency sweep for a bridge microbeam with biomolecules is shown in Figure 4. For the data shown, the frequency after cleaning is 126.8 kHz. The frequency shifts downward to 126.0 kHz when avidin is attached to the surface. The frequency shifts further down to 124.7 kHz with the biotin(-avidin pair). The net change in resonant frequency is 1.6%. For a monolayer of avidin/biotin ($\gamma_a=6.64E-16 \text{ g/m}^2$ and $\gamma=2.55E-11 \text{ g/m}^2$) the frequency shift (equation 3) will be 0.0013%. A resonant frequency shift of 1.6% corresponds to an added mass that is approximately 3.3% of the mass of the beam ($\gamma_a=8.5E-13 \text{ g/m}^2$).

The data obtained by introducing a biotin/fluorescein are shown in figures 5. The intensity of the fluorescein is inversely related to the shift in frequency. As the frequency drops, indicative of added mass, the intensity of fluorescence increases. The data in figure 5 confirm that the shift in resonant frequency is related to the added mass of the biomolecule.

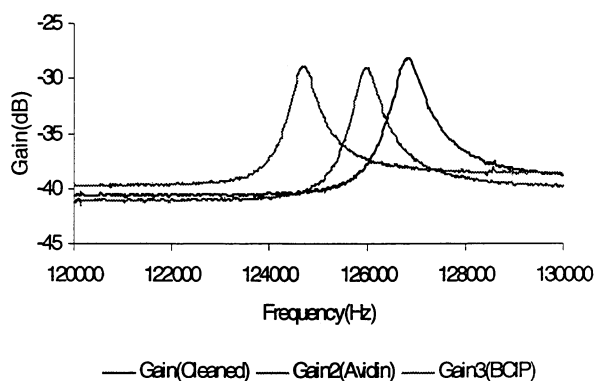


Figure 4: Frequency sweep data for a microbeam that has been immersed in solutions of Avidin and Biotin. As each material is added the resonant frequency is lowered.

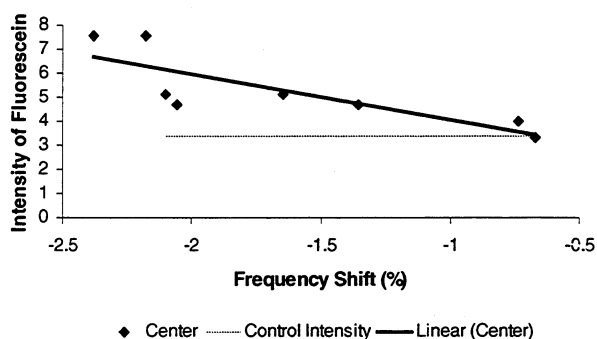


Figure 5: Intensity of the fluorescence as a function of frequency shift in bridge devices.

5 CONCLUSION

In this study, the suitability of MEMS microbeams as a drug screening tool was investigated. PZT-actuated cantilever and bridge structures were fabricated and tested. The tests focused on measuring the shift in resonant frequency of the beams when a biomolecule is attached to the beam. Test data indicate that resonant frequencies of bridge structures are much close to theoretical predictions than cantilever beam structures. However, the bridge structures are stiffer, reducing the number of resonant frequencies that can be detected. The addition of a biomolecule does lower the resonant frequency by 1 to 2%. This shift is much larger than anticipated for the mass associated with a monolayer of avidin/biotin. Experiments with fluorescent microscopy support the conclusion that the downward shift in resonant frequency is related to the added mass of the biomolecule. These experiments show that small masses can be detected with microscale structures.

REFERENCES

- [1] D. A. Walters, J. P. Cleveland, N. H. Thomson, P. K. Hansma, M. A. Wendman, G. Gurley, and V. Elings, "Short Cantilevers for Atomic Force Microscopy", *Rev. Sci. Instrum.* 67, 3583 (1996).
- [2] G. Y. Chen, R. J. Warmack, T. Thundat, D. P. Allison, and A. Huang, "Resonance Response of Scanning Force Microscopy Cantilevers", *Rev. Sci. Instrum.* 65, 2532 (1994).
- [3] T.E.Schaffer, J.P.Cleveland, F.Ohnesorge, D.A.Walters, P.K.Hansma, "Studies of vibrating atomic force microscope cantilevers in liquid", *J. Appl.Phys.*80 (7), 3622, (1996).
- [4] R.J. Roark, and W. Young. *Formulas for Stress and Strain*, McGraw-Hill Book Co., New York, (1975).
- [5] D. Polla, P. Schiller, and L. Francis, "Microelectromechanical systems using Piezoelectric Thin Films," *Proc. SPIE Integrated Optics Microstructures II*, vol. 2291, 108-124, (1994).